Soft Matter



View Article Online PAPER



Cite this: Soft Matter, 2016, **12**, 5304

Received 14th March 2016 Accepted 12th May 2016

DOI: 10.1039/c6sm00637j

www.rsc.org/softmatter

Polyelectrolyte/surfactant films spread from neutral aggregates

Richard A. Campbell.* Andrea Tummino. Boris A. Noskov and Imre Varga*

We describe a new methodology to prepare loaded polyelectrolyte/surfactant films at the air/water interface by exploiting Marangoni spreading resulting from the dynamic dissociation of hydrophobic neutral aggregates dispensed from an aqueous dispersion. The system studied is mixtures of poly(sodium styrene sulfonate) with dodecyl trimethylammonium bromide. Our approach results in the interfacial confinement of more than one third of the macromolecules in the system even though they are not even surface-active without the surfactant. The interfacial stoichiometry of the films was resolved during measurements of surface pressure isotherms in situ for the first time using a new implementation of neutron reflectometry. The interfacial coverage is determined by the minimum surface area reached when the films are compressed beyond a single complete surface layer. The films exhibit linear ripples on a length scale of hundreds of micrometers during the squeezing out of material, after which they behave as perfectly insoluble membranes with consistent stoichiometric charge binding. We discuss our findings in terms of scope for the preparation of loaded membranes for encapsulation applications and in deposition-based technologies.

Introduction

Oppositely charged polyelectrolyte/surfactant (P/S) mixtures have generated interest for more than one hundred years, primarily because of the huge commercial value of the formulations we use in our everyday lives. 1-3 Their properties at the air/water interface have been the focus of several substantial bodies of work over the last decades, the results of which were typically set in the context of P/S co-adsorption or complex adsorption at equilibrium.⁴⁻⁶ The equilibrium bulk phase behavior of these systems has been thoroughly investigated as well, and can comprise a two phase region where complexes with low charge lack colloidal stability and aggregate, precipitate and either sediment or cream.⁷⁻⁹

Recent work on non-equilibrium effects in the bulk has shown that aggregates produced in the two phase region that are then diluted to the one phase region, e.g., due to concentration gradients present during mixing, can persist over extended time scales as a result of their kinetic charge stability. 10-12 It has also been shown that aggregate production can have important effects at the air/water interface. Either there can be depletion of the

amount of material due to a reduction in the concentration of surface-active material in the bulk^{13,14} or enhancement by a

sulfate (PEI/SDS) mixtures, it was shown using the expanding liquid surface of an overflowing cylinder that the dissociation of aggregates on a sub-second time scale results in the formation of transient monolayer patches by Marangoni spreading. 17 It was inferred that under dynamic conditions relevant to processing and applications even more polyelectrolyte can be delivered to the interface by the spreading of material from aggregates than by the adsorption of molecular components. In another study on poly(amido amine) dendrimer/SDS mixtures, it was demonstrated that only aggregates with sufficient charge became embedded intact in the interfacial layer. 18 It was inferred that the aggregates closer to charge neutrality, more abundant in the two phase region yet not detected intact at the interface, must dissociate and spread material upon contact with the surface layer. As the equilibrium state in the two phase region is complete precipitation, ⁷⁻⁹ with coagulation of the aggregates taking up to several weeks or even longer, 10,14 their fast, spontaneous dissociation at the air/water interface highlights the important role of surface forces in the dynamic spreading process.

The spreading process is thermodynamically favorable as the self-assembly of amphiphilic material at the air/water interface lowers its free energy. Equally, thermodynamics predicts

range of different direct non-equilibrium interactions. 15,16 The key roles that P/S aggregates can play in determining the properties of the air/water interface have been recently highlighted. In one study on poly(ethylene imine)/sodium dodecyl

^a Institut Laue-Langevin, 71 Avenue des Martyrs, CS20156, 38.042 Grenoble Cedex 9, France. E-mail: campbell@ill.eu; Tel: +33 476 207 097

^b Institute of Chemistry, Eötvös Loránd University, Budapest 112, P. O. Box 32, H-1518 Hungary. E-mail: imo@chem.elte.hu; Tel: +36 204 890 440

^c Institute of Chemistry, St. Petersburg State University, 198904 St. Petersburg,

Paper

that that in equilibrium the bulk chemical potential of the P/S complexes in solution is finite, hence some of the polymers should dissolve in the solution. Nevertheless, kinetic barriers to the dissolution can result in the trapping of material at the interface in the form of loaded surface films. Exploitation of non-equilibrium effects to create loaded films of macromolecules dates back to almost one century with work on spread protein films. 19,20 In the following decades, studies of spread films of amphiphilic macromolecules became an important field of interface science. 21,22 More recently, some groups have studied the dynamic properties of adsorbed P/S layers with Jain et al. noting the possibility of compressing them.²³ Bergeron et al. later commented on their gel-like behavior²⁴ and Noskov et al. described their surface heterogeneities.²⁵ Edler et al. went on to work extensively on film formation in mixtures of PEI with surfactants of the same charge.²⁶

Approaches to control the interfacial properties of P/S mixtures by tuning the experimental pathway have been recently employed. For example, Dhar et al. described the preparation of films from refined P/S nanoparticles, 27,28 while Tong et al. reported the interfacial disassembly of positively charged P/S nanoparticles triggered by particle-particle interactions.²⁹ Also, Lee et al. formed stable films of poly(sodium styrene sulfonate) and alkyltrimethylammonium bromides of different chain lengths by spreading a small aliquot of mixed solution in an organic solvent.³⁰ In that work, the interfacial stoichiometry of the films was resolved following their transfer to a mica substrate. Even so, quantitative information on the interfacial stoichiometry in situ at the air/water interface during dynamic measurements has been limited by the accuracy and kinetic resolution of measurements using the available experimental techniques.

Complementary to the methodologies employed to date, in the present work we exploit explicitly the rapid dissociation of hydrophobic neutral P/S aggregates present in an aqueous dispersion to create loaded films by Marangoni spreading. The loaded films are more efficient than layers formed by bulk adsorption in terms of the ratio of the surface excess to the amount of material used. This may have certain economic and environmental advantages, and the preparation of such films using only aqueous media include reduced cost and toxicity as well as potential for biocompatibility. The system studied is poly(sodium styrene sulfonate)/dodecyl trimethylammonium bromide (NaPSS/DTAB). It was chosen to emphasize the significance of spreading from neutral aggregates, which are produced at bulk compositions far from stoichiometric charge mixing. A powerful new implementation of neutron reflectometry with superior kinetic resolution and accuracy in the interfacial stoichiometry than has been previously achieved is applied in situ during dynamic measurements for the first time to reveal the high robustness of the films created.

Experimental section

Materials

Pure H₂O was made by passing deionized water through a Milli-Q purification system (total organic content = 4 ppb; resistivity = 18 m Ω cm). Dodecyltrimethylammonium bromide (DTAB; Sigma; ≥98%) was recrystallized twice in a 4:1 mixture of acetone to ethanol, and each time the solutions were cooled over a few hours to maximize the purity. D_2O (Aldrich, > 99.9 atom% D), deuterated DTAB (dDTAB; CDN Isotopes; 98.7 atom% D) and poly-(sodium styrene sulfonate) (NaPSS; Sigma Aldrich; $M_W = 17$ kDa; $M_{\rm W}/M_{\rm N} \approx 1.1$) were all used without further purification.

Sample preparation

Spread films were formed by dispensing droplets of a concentrated aliquot containing a dispersion of NaPSS/DTAB aggregates at various positions above a pure water surface using an Eppendorf pipette angled at $\sim 45^{\circ}$ with a dropping height of ~ 5 mm. The aliquots comprised 100 ppm NaPSS freshly mixed with 6 mM DTAB in pure water. The mixing procedure was performed according to the 'standard mixing' protocol of Tonigold et al.31 where equal volumes of polyelectrolyte and surfactant solutions at double their final concentrations, i.e., 200 ppm NaPSS with 12 mM DTAB, were poured together simultaneously into a freshly cleaned vessel. The mixture was always dispensed within 1 min after mixing. The surfactant used was DTAB in all experiments except for neutron reflectometry (NR) where either dDTAB or contrast matched DTAB (cmDTAB) was used, the latter comprising 4.4% by volume dDTAB in DTAB. The pure water used was H2O in all experiments except for NR where air contrast matched water (ACMW) was used, comprising 8.1% by volume D2O in H2O. Experiments performed in a static dish involved 100 µL of the NaPSS/DTAB solution dispensed on 25 mL of pure water; the circular dish had a diameter of 6.9 cm. Those performed in a Langmuir trough (NIMA, Coventry, UK) involved 500 µL of NaPSS/DTAB solution dispensed on 125 mL of pure water; the trough had an area of $10 \text{ cm} \times 13.3-28.3 \text{ cm}$ depending on the barrier positions. The surface pressure was measured using a Wilhelmy plate made of filter paper over 5 compression/expansion cycles. The barrier speed was 6.2 mm min⁻¹ resulting in a cycle time of 24 min.

Adsorbed layers were formed in a static trough by mixing equivalent amounts of materials in a different way. First, 100 μL of 200 ppm NaPSS was diluted in 25 mL of pure water to make 0.8 ppm solution, and 100 μL of 12 mM DTAB was diluted in 25 mL of pure water to make 48 μM solution. These solutions were then poured together simultaneously into a freshly cleaned vessel. Then 30 mL was poured into the dish, and around 5 mL was aspirated using a suction pump, which was essential to remove any kinetically-trapped material. 15,16,31 All the measurements were carried out at 25 °C.

Electrophoretic mobility

The electrophoretic mobility of the complexes in freshly-mixed NaPSS/DTAB solutions was measured to characterize their charge and determine the point of charge neutrality. A Malvern Zetasizer NanoZ instrument was used on the basis of the M3-PALS technique. The standard error in the values of the electrophoretic mobility was around 10%.

UV-vis spectroscopy

The turbidity of freshly mixed NaPSS/DTAB solutions was measured to characterize the extent to which macroscopic aggregates Soft Matter Paper

were suspended in the bulk solution. A Perkin-Elmer Lambda 2 UV-vis spectrophotometer with a semi-micro quartz cell having a 1 cm path length was used. In each case the optical density of the samples was determined at 400 nm (O.D.400). Measurements were carried out 5 min after mixing. Since neither the polyelectrolyte nor the surfactant has an adsorption band above 350 nm, the increasing O.D.400 values indicate the presence of the aggregates.

Dynamic light scattering (DLS)

DLS measurements were performed using a Brookhaven 200SM goniometer, a BI-9000AT high speed correlator and a 1 W Argon ion laser operating at 488 nm. The measured correlation function was evaluated by cumulant analysis and the CONTIN method. The apparent hydrodynamic diameters were calculated from the determined diffusion coefficient using the Stokes-Einstein equation. The results from the two methods were consistently in good agreement indicating the reliability of the measurements.

It should be noted that due to the large scattering crosssection of the formed aggregates, the freshly mixed samples exhibited multiple scattering and we could not measure them directly. To overcome this problem, we took samples at regular intervals and diluted them tenfold to reduce multiple scattering. This was possible because the samples contained neutral aggregates where the amount of surfactant bound to the polyelectrolyte is equal to the monomer concentration of the polyelectrolyte, and therefore the equilibrium free surfactant concentration was precisely determined (5.5 mM DTAB). Practically, this meant that the dilution of the samples with 5.5 mM DTAB did not affect the surfactant chemical potential or the extent of surfactant binding, and therefore the physical state of the aggregates was preserved.

Ellipsometry

Ellipsometry measurements were made on NaPSS/DTAB films spread from aggregates on pure water and layers of NaPSS/ DTAB adsorbed from solution each contained in a static trough. They are based on the change in polarization of light reflected at an interface in the 1 mm² area illuminated by the laser beam. The p- and s-components of the reflectivity change by different amounts according to the dielectric properties of the interface. The sensitivity of the phase shift (Δ) is much greater than the amplitude change to the amount of interfacial material for thin, non-absorbing layers at the air/water interface, so only the former variable was analysed.

There are various different approaches in the literature to calculate the surface excess (Γ) from the measured values of Δ . An optical matrix model can be used to derive either a linear relation for an oil-like layer (i.e. constant density with changing thickness) or a quadratic relation for a particle-like layer (i.e. constant thickness with changing density). However, it is often considered better to calibrate the relation with reference to a direct measure of the surface excess from a technique such as neutron reflectometry. 32,33 We opted for the latter approach, given that the interfacial stoichiometry of a spread film was measured directly using this technique, and hence we had

already a direct measure of the total surface excess. This scaling for sample A, a spread film of equimolar interfacial stoichiometry where counterions are assumed not to be present at the interface, was then also applied to samples B-E. The presence of any counterions at the interface in those samples would mean that the actual surface excesses are in fact slightly lower than the values reported, but this does not affect our interpretations of the data. A Beaglehole Picometer Light ellipsometer was used with a wavelength of $\lambda = 632.8$ nm, an angle of incidence of $\theta = 50^{\circ}$, and a data acquisition rate of 0.2 Hz.

Neutron reflectometry (NR)

NR measurements were made on NaPSS/DTAB films spread from neutral aggregates on pure water prior to and during dynamic compression/expansion cycles on a Langmuir trough. They are based on the scattering excess of neutrons reflected off a layer at the surface of ACMW. The scattering excess is determined by a convolution of the amount of material at the interface and its scattering properties, the latter of which can be tuned by changing the isotopic composition. The measurements are of the specular reflection of neutrons with respect to the wave vector transfer normal to the interface, Q_z , given by

$$Q_z = \frac{4\pi \cdot \sin \theta}{\lambda} \tag{1}$$

Measurements were performed on the horizontal time-of-flight reflectometer FIGARO at the Institut Laue-Langevin (Grenoble, France).³⁴ A high flux instrument configuration was used with $\theta = 0.62^{\circ}$ and de-phased choppers giving pulses with a wavelength resolution of 9.0–9.6% $d\lambda/\lambda$ in the range $\lambda = 2-16$ Å. Only data in the range 4.5-14 Å were used in the analysis, which corresponds to a Q_z range of 0.01–0.03 Å⁻¹. Background was not subtracted from the data, and the analysis was carried out using the batch fitting feature of Motofit.35

NR has been used extensively to resolve the interfacial stoichiometry of binary mixtures at the air/water interface by fitting a common physical model to experimental data recorded in different isotopic contrasts of the surface material and solvent. 6,13,14,36-40 However, even at leading instruments today, the measurements take typically up to a couple of hours in total as data are required in multiple isotopic contrasts across a broad range of Q_z values where the reflectivity values descend to ppm levels. As such, resolution of the interfacial stoichiometry of a mixture at the air/water interface during surface area cycles has not been achieved to date. A further limitation of this approach is that the layer roughness values used in the model have an impact on the derived polyelectrolyte surface excess values, yet they are a priori unknown, limiting the accuracy of the measurement.

In the present work, we resolve directly the interfacial stoichiometry much faster and more accurately than in previous studies (in the absence of deuterated polyelectrolyte) using a recent approach 14,41 that has been applied to a dynamic system for the first time. The approach is based on the sequential acquisition of data recorded only at low Q_z values in two isotopic contrasts: (1) NaPSS with dDTAB in ACMW, where the strong scattering is dominated by the deuterated surfactant, and (2) NaPSS with

Paper

-2.0 -2.5 -3.0 -3.5 -4.5 -5.0 -5.5 -

Fig. 1 Examples of neutron reflectivity profiles of spread NaPSS/DTAB films on a Langmuir trough prior to compression with (red) dDTAB recorded for 1 min, (blue) cmDTAB recorded for 2 min; (green) bare ACMW recorded for 2 min.

0.020

Q (Å⁻¹)

0.025

0.030

0.015

0.010

cmDTAB in ACMW, where the very weak scattering is determined only by the amount of polyelectrolyte. The approach exploits the high flux at low Q_z values accessible on the FIGARO instrument. The data were binned to 1 min slices for contrast 1 and 2 min slices for contrast 2, as a result of the difference in magnitudes of the measured reflectivities. These two scattering excesses are then resolved using linear equations into both the polyelectrolyte and surfactant surface excesses. Examples of the experimental data and model fits are shown (Fig. 1).

The physical basis of the approach is described below. The surface excess of a single-component monolayer at the air/ACMW interface may be determined using 42

$$\Gamma = \frac{\sigma \cdot d}{b_i \cdot N_{\rm A}} \tag{2}$$

where $\sigma \cdot d$ is the product of the scattering length density and layer thickness of a uniform layer at the air/water interface, b_i is the scattering length of the molecule i (which is related to the sum of coherent scattering cross sections for all the atoms present in the molecule), and $N_{\rm A}$ is Avogadro's number. Here the values of b_i = 47.6 fm for NaPSS and 242.2 fm for DTAB were used; note that the data indicate stoichiometric binding at the interface so contributions from the counterions were neglected from this calculation. If one combines additively the contributions of the two components of the layer (i = 1, 2) in the product $\sigma \cdot d$, eqn (2) takes the form

$$\sigma \cdot d = N_{\mathbf{A}} \cdot (\Gamma_1 \cdot b_{i,1} + \Gamma_2 \cdot b_{i,2}) \tag{3}$$

Here NaPSS/DTAB mixtures in the two isotopic contrasts stated above result in the following two linear equations:

$$(\sigma \cdot d)_1 = N_{A} \cdot (\Gamma_{\text{surf}} \cdot b_{i,\text{d-surf}} + \Gamma_{\text{poly}} \cdot b_{i,\text{poly}}) \tag{4}$$

$$(\sigma \cdot d)_2 = N_A \cdot \Gamma_{\text{poly}} \cdot b_{i,\text{poly}} \tag{5}$$

These linear equations may then be solved to determine Γ_{poly} and Γ_{surf} . It is not important which one of σ and d is fixed and which one is fitted: in this case we fitted d having fixed $\sigma = 3.0 \times 10^{-6} \text{ Å}^{-2}$ with layer roughness values of 4 Å. Two factors, however, are critical for the success of this approach. First, the data must be fitted only at low Q_2 values so that the model is made insensitive to the actual structure present at the interface. For example, if σ is halved or doubled in the fitting of contrast 1 to the (red) data in Fig. 1, the fitted product $\sigma \cdot d$ changes only by $\sim 1\%$; note that these extra fits all overlap visually and so for clarity are not displayed. Furthermore, changing the layer roughness values in the range 3-5 Å, which would have had a large impact on Γ_{poly} using the traditional NR approach, changes the product $\sigma \cdot d$ by < 0.3%. Second, accurate quantification of Γ_{poly} relies on the correct determination of the background for inclusion in the model. Here, a series of measurements of a bare air/ACMW interface were made over the same acquisition time that was used for the analysis of the NaPSS/DTAB data. The minimum value of the background that allowed convergence to zero surface excess of fitting a fictitious layer of an arbitrary finite scattering length density on its surface was determined to 3 significant figures. The average values of 15 measurements of 1 min were used for contrast 1 (background = 2.30×10^{-5}) and 7 measurements of 2 min were used for contrast 2 (background = 1.71×10^{-5}). The interfacial material in the NaPSS/DTAB measurements was then determined precisely from the scattering excess measured above the calibrated background.

Brewster angle microscopy (BAM)

BAM measurements were made on a film of NaPSS/DTAB spread from neutral aggregates on pure water during the first dynamic compression/expansion cycle on a Langmuir trough. The measurements provide a representation of lateral heterogeneities in the interfacial structure on the micrometer scale. They were made at the Brewster angle for the air/water interface of 53.1° using a Nanofilm EP3 machine equipped with an NdYAG laser and a $10\times$ objective. Automatic focusing was disabled due to the dynamic nature of the film. Gamma correction was applied equally to all images to emphasize the faint features observed.

Results and discussion

Prior to a description of our work on spread P/S films formed by exploiting the dissociation of neutral aggregates, first it is necessary for us to understand the bulk binding, phase behavior and size distributions in the aggregate dispersions that will be used. Electrophoretic mobility and optical density data are presented for samples with a fixed NaPSS concentration of 100 ppm and different DTAB concentrations (Fig. 2). Even though the bulk composition of stoichiometric mixing of polyelectrolyte and surfactant charges involves just 0.48 mM DTAB, 6 mM is required to produce neutral aggregates, as indicated by the vertical black arrow. This excess may be related to factors such as the strength of electrostatic interactions and the polyelectrolyte

Soft Matter Paper

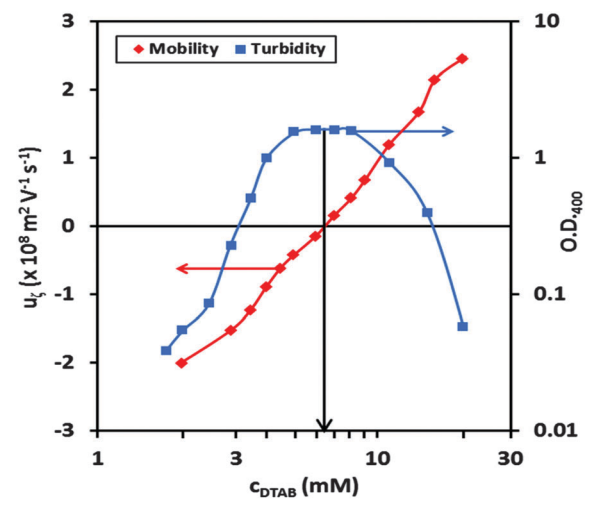


Fig. 2 Electrophoretic mobility data of freshly mixed NaPSS/DTAB samples, and optical density data measured at 400 nm. Lines joining the data are only to guide the eye.

chain flexibility.⁴³ The maximum of the turbidity data indicates that the formation of aggregates is optimal at the same bulk composition.

DLS data are presented for samples with 100 ppm NaPSS and 6 mM DTAB with respect to the sample age (Fig. 3). It can be seen that the size of the aggregates is already ~ 500 nm immediately after mixing. The size then increases continuously with further aggregation and after 10 min it reaches 1000 nm. We determined the evolution of the particle size distribution during this early aggregation state using the CONTIN method.

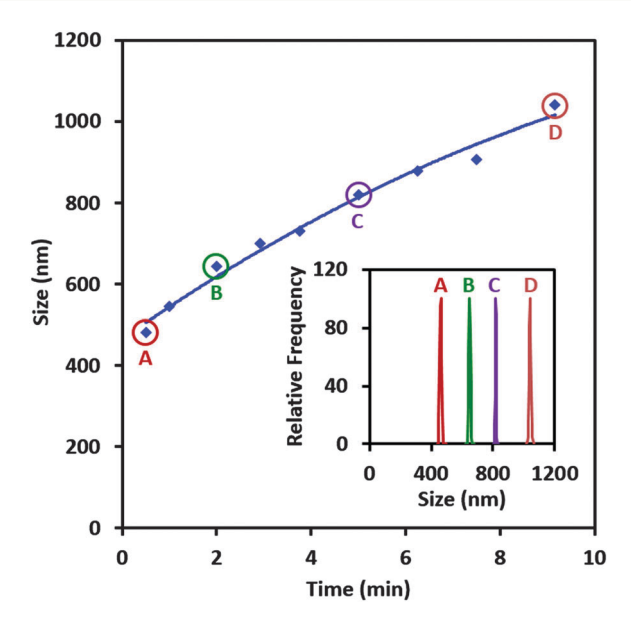


Fig. 3 Dynamic light scattering data of the average hydrodynamic diameter (size) of NaPSS/DTAB aggregates with respect to the sample age (time); the inset shows the size distributions of 4 samples as labelled in the main panel. The line joining the data is only to guide the eye. Note that the mixtures were diluted with 5.5 mM DTAB solution to reduce multiple scattering, a procedure that did not change the physical state of the aggregates (see Experimental section).

We found narrow unimodal particle size distributions in all cases. In the experiments that follow we dispense P/S aggregates on a clean water surface within the first minute after mixing the components; hence we may infer that the samples contained aggregates with a well-defined size distribution of 500 ± 50 nm. As such, the samples used comprised a dispersion of aggregates that had not precipitated nor were separated from the supernatant. Note that while the internal structure of the NaPSS/DTAB aggregates was not investigated in the present work, Sitar *et al.* presented data on the phase diagram of the PSSDTA/water system and found that above 43% water content coexisting hexagonal ('precipitate') and micellar ('dilute') phases form. 44

We begin our focus on the interfacial properties by examining how the dissociation of neutral P/S aggregates can be used to create spread films. Thus, we spread a small aliquot (100 $\mu L)$ of a freshly prepared mixture containing neutral aggregates (100 ppm NaPSS and 6 mM DTAB) on 25 mL of pure water using a pipette. Ellipsometry was used to measure the surface excess for 1 h. Even though the final concentrations were just 0.4 ppm NaPSS and 24 μM DTAB, a substantial spread film is immediately formed with its surface excess remaining practically constant throughout the measurement (Fig. 4; sample A). While there is excess surfactant present in the aliquot, adsorption from an equivalent amount in the absence of NaPSS results in only a minimal adsorbed layer (Fig. 4; sample E). These results highlight the key role of NaPSS in the spread film.

Next we compared the efficiency of aggregate spreading with the adsorption of P/S complexes from the bulk. We prepared a mixture directly in the one-phase region with 0.4 ppm NaPSS and 24 μM DTAB (free of aggregates) by mixing previously-diluted components in a stoichiometric charge ratio. The adsorbed layer

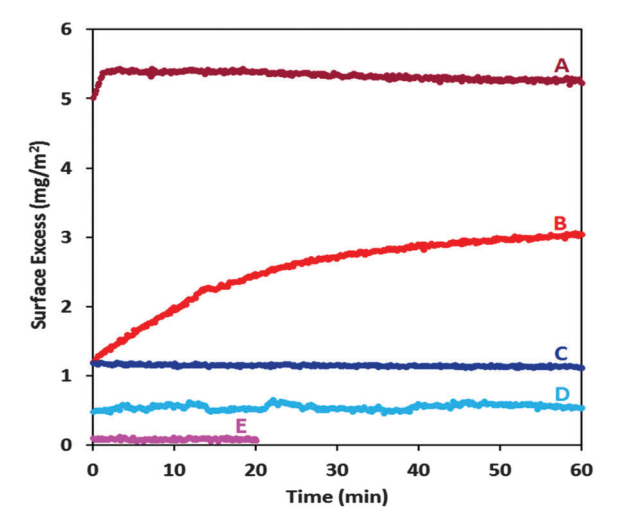


Fig. 4 Ellipsometry measurements of the total surface excess of NaPSS and DTAB where the values are scaled to that of sample A measured directly using NR; the presence of any counterions in samples B–E would mean that the surface excesses are slightly overestimated. Samples A and C are spread films while samples B and D are the respective adsorbed layers with equivalent amounts of the components; the spread films were prepared using 100 μL aliquots of 100 ppm, 17k NaPSS with (A) 6 mM and (C) 0.4 mM DTAB dispensed on 25 mL of pure water in a static trough; sample E is the average of 3 repeats of A in the absence of NaPSS.

Paper

only slowly forms, approaching a lower steady state surface excess (Fig. 4; sample B). Although the mixtures in samples A and B each contain the same total concentrations of NaPSS and DTAB, the initial surface excess is four times higher in the case of the film spread from neutral aggregates. This result highlights the non-equilibrium nature of the spreading process by exploiting aggregate dissociation.

Lastly, we carried out experiments on spread and adsorbed layers where aggregates were absent in both cases: the DTAB concentration in the aliquot was decreased to 0.4 mM (Fig. 4; samples C and D). It may be noted that this bulk composition is close to that of stoichiometric mixing of the polyelectrolyte and surfactant charges, which is a common reference point in literature studies of P/S systems. 9,45 In this case, the resulting surface excess is much smaller than for the film spread from neutral aggregates, which emphasizes the importance of aggregate dissociation in the kinetic-trapping of material at the interface.

We go on now to examine the dynamic properties of the spread films during 5 compression/expansion cycles on a Langmuir trough (Fig. 5). Following an increase in surface pressure during the 1st cycle, the values reach a plateau, which corresponds to the minimum surface tension of 44 mN m⁻¹ for the NaPSS/DTAB system.36

There is a large hysteresis upon expansion only during the first cycle, after which lower surface pressures are achieved during expansion, possibly due to squeezing out of material from the interface. The system approaches a limit cycle with minimal hysteresis in subsequent cycles, which may suggest that the material is trapped at the interface in an insoluble membrane. Quantification of the amounts of the components at the interface, however, would be required to qualify such statements. Therefore we applied our new NR approach to resolve the interfacial stroichiometry of binary mixtures (described above) to dynamic P/S films in situ

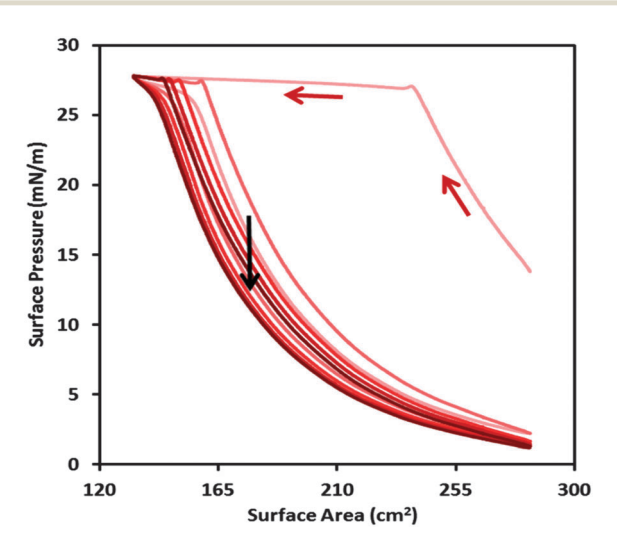


Fig. 5 Langmuir isotherms of 5 cycles of NaPSS/DTAB films spread from neutral aggregates as described in the main text where each cycle is displayed progressively darker in shading; the progression of the data with time is indicated generally by the black arrow and specifically during the first compression by the red arrows

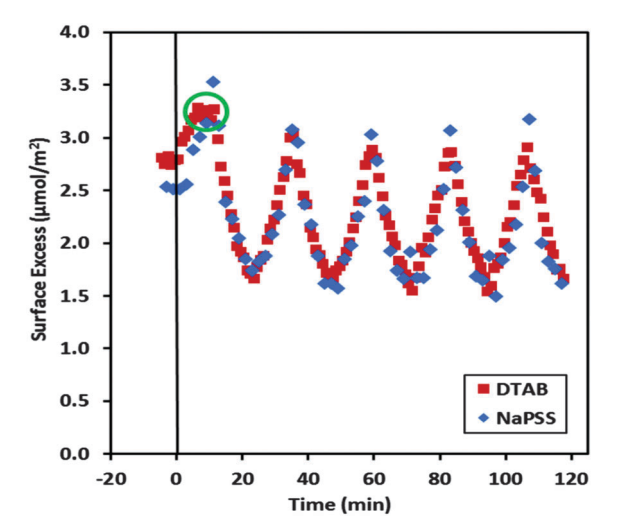


Fig. 6 Interfacial stoichiometry of NaPSS/DTAB films spread from neutral aggregates resolved using NR where the maxima mark full compression and minima mark full expansion corresponding to the surface area cycles in Fig. 5: the deviation of the interfacial stoichiometry from unity prior to and during the first compression is attributed to differences in the spreading dynamics of NaPSS/DTAB aggregates of different isotopic contrasts, which is reset when the films are compressed beyond a complete surface layer.

for the first time. Data from the 5 compression/expansion cycles are presented (Fig. 6).

A striking observation is the consistent stoichiometric charge binding at the interface after the first compression. Such a stoichiometry could be expected for this system since it represents the lowest surface energy state while keeping the material at the interface charge neutral. The adsorption of excess surfactant resulting in electric double layer formation and the accumulation of polyelectrolyte loops are both energetically unfavorable given the very low bulk surfactant concentration and ionic strength. In fact this interfacial picture was inherent in the equilibrium co-adsorption model for oppositely charged flexible P/S mixtures proposed by Asnacios et al. two decades ago.5 Such an interfacial stoichiometry was also previously resolved by Lee et al. using X-ray photoelectron spectroscopy on NaPSS/alkyltrimethylammonium bromide films that were first spread on water from a dispersion in an organic solvent and then deposited onto a mica substrate.²⁸ However, the present work marks the first time that stoichiometric binding has been convincingly demonstrated in situ at the air/water interface both for static P/S films and for films subjected to dynamic perturbations of the surface area.

Our accurate approach to resolve the dynamic interfacial stoichiometry of binary mixtures is clearly much faster than was previously possible, and is suitable for application in a range of systems where the interfacial stoichiometry is totally unknown. Indeed work is underway already to determine the properties of films created by aggregates with a range of compositions and ionic strengths. The latter variable is particularly important given that this is a key parameter to tune to balance between equilibrium and non-equilibrium behavior. 46,47 As one looks to future advances in neutron instrumentation, such as the

Soft Matter

RAINBOWS⁴⁸ upgrade planned for the FIGARO instrument where at least another order of magnitude in flux is anticipated from the use of a dispersive beam, resolution of the dynamic insertion of macromolecules in biological interfacial films on time scales relevant to respiration seems soon to be a realistic

prospect.49,50 During the first compression, the plateau in the surface pressure is accompanied by one in the surfactant surface excess (see green circle in Fig. 6). We can conclude therefore that material is indeed expelled from the film as the complete surface film is compressed further. Interestingly, Brewster angle microscopy images indicate a change in the morphology of the film only during the squeezing out process (Fig. 7). In contrast to images prior to the surface pressure plateau (A) and during expansion (C), which are black due to the low optical contrast of the film, the image during the squeezing out process (B) has faint linear white features indicating ripples with a length scale on the order of hundreds of micrometers. This effect cannot be connected with the propagation of longitudinal surface waves because the corresponding dispersion relation leads to wavelengths much longer than the trough length at low frequencies < 0.01 Hz. 51 It is more probable that the ripples are due to the film buckling like in the case of layers of polystyrene microparticles at the air/water interface close to the collapse state.⁵² It is likely that the lower regularity of the ripples in the present work is connected with the distortion related to buckling of the film when the material is squeezed out of the interface. Interestingly, the surface excess values after each expansion are constant but lower than the starting value. As such, we may conclude that the surface excess is effectively reset after the first compression when any material in excess of a complete surface layer is eliminated from the interface.

Following the first compression, the interfacial excess and stoichiometry are highly reproducible during the cycles. Since no decrease in the surface excess is observed over the course of the repeated cycles, we may infer that the spread films are effectively insoluble on the investigated time scales and their behavior is similar to that of the monolayers of insoluble surfactants. This result has an important implication. While the polyelectrolyte at 100 ppm is not even surface active alone, 64 of the total amount in the system is confined in the spread films using our approach; we note that this efficiency may be increased further by optimization of the spreading process. In comparison with techniques like electrospray deposition, 55

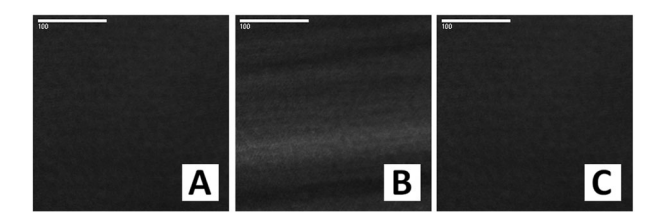


Fig. 7 Brewster angle microscopy images of NaPSS/DTAB films spread from neutral aggregates recorded during compression at surface areas of (A) 260 cm² and (B) 160 cm², and (C) during expansion at a surface area of 210 cm². The scale bar represents 100 micrometers in each case.

such a method could be a more efficient and cheaper way to generate thin amphiphilic films for transfer, and there is scope for encapsulation of hydrophobic additives, such as drugs or dyes, in the films.⁵⁶ This way to produce loaded amphiphilic films could also result in reduced environmental impact in certain applications.⁵⁷ As the basis of our approach was built on recent studies of a number of different systems,^{13–18} it follows that there is capacity for its general exploitation with the choice of macromolecule tailored to the spreading characteristics of the target molecule to be released.

Lastly, it should be mentioned that different interpretations have been proposed in the literature for the behavior of the NaPSS/DTAB system at the air/water interface. Taylor et al. assumed that the interfacial layer is in dynamic equilibrium with the aqueous bulk phase following the adsorption of molecular components hence the interfacial properties are determined by bulk chemical potentials, 38 and thermodynamic models within a framework of chemical equilibrium were later applied to the data.58,59 (Note that recent discussions revealed that these samples were freshly diluted using NaPSS solution shortly before their measurement so as a result of the high free surfactant concentration in the two phase region they must have inevitably contained a dispersion of aggregates far from equilibrium. 60) In contrast, Lee et al. showed that NaPSS/alkyltrimethylammonium bromide mixtures spread as molecular dispersions from an organic solvent form films that are practically insoluble on experimentally accessible time scales, although we note that they used a higher molecular weight (70 kDa) polyelectrolyte.³⁰ In the present work, we have advanced this understanding in a number of respects. First, we have outlined a methodology to exploit the dynamic dissociation of hydrophobic neutral aggregates formed in the aqueous bulk to create loaded films at the air/water interface by Marangoni spreading. This result is significant in terms of film preparation approaches given that water is cheaper and less toxic than organic solvents. Second, we found that even the lower molecular weight (17 kDa) NaPSS can form insoluble films with DTAB at the air/water interface. Indeed in spite of fast equilibration of the interface, as the surface film is formed on a sub-second time scale, there is an extreme lack of equilibration between the interfacial film and the bulk, which persists at least for minutes and hours, not only under static conditions but also under the dynamic conditions relevant to processing and applications. This result implies that the application of equilibrium models to experimental data for oppositely charged P/S systems must be carried out with great caution, especially given how any aggregates present in the samples can dissociate and spread material at the interface under equilibrium conditions. Third, by utilizing a new implementation of neutron reflectometry, we determined that stoichiometric charge binding is characteristic of NaPSS/DTAB films on a dilute aqueous subphase under both static and dynamic conditions. We believe that a comparison of this behavior with films prepared from aggregates of different charges and using different ionic strengths of the bulk can lead to the optimized preparation of films with a range of different properties in the future.

Paper Soft Matter

The application of our new methodology to other P/S systems is straightforward: one simply has to determine the point of zero aggregate charge in the bulk (electrophoretic mobility) and an aliquot containing a dispersion of fresh hydrophobic neutral aggregates can then be used. Even so, the factors that affect the efficiency of the spreading mechanism in different systems (e.g. polymer size, molecular weight and architecture, ionic strength, surfactant properties and the aggregate internal structure) are exciting topics for future investigations.

Conclusions

Oppositely charged P/S mixtures have been studied extensively over the years with the results often interpreted within a framework of chemical equilibrium. Recent work has revealed the strong effects that bulk aggregation can have on the interfacial properties as well as the range of different non-equilibrium processes that affect the interfacial properties on experimentally accessible time scales. Various attempts have been made to study the film-like properties of these mixtures by modifying the experimental pathway such as spreading complexes in carrier solvents. In the present work, we have outlined a simple methodology to form loaded spread films by exploiting explicitly the dissociation of hydrophobic neutral aggregates at the air/water interface.

Using the NaPSS/DTAB system as an example, we have shown that these films can result in the interfacial confinement of more than one third of the polyelectrolyte in the system. Even though the surface excess never exceeded that of a complete surface layer of each component, the value of our methodology is related to the efficiency of the surface loading, i.e., a substantial surface excess can be achieved by using only a minimal amount of material in comparison with a system relying on bulk adsorption. The dynamic properties of the films were examined using a new implementation of neutron reflectometry, which enhanced the accuracy and time resolution of the interfacial stoichiometry measured in situ during dynamic surface area cycling for the first time. Consistent stoichiometric charge binding at the interface was observed, and following the squeezing out of excess material beyond that of a complete surface layer during the first compression the material at the interface was conserved during subsequent cycles. The films behave subsequently like perfectly insoluble membranes. These results revealed the potential to set the coverage of the films simply by tuning the dynamic surface area, which has been only inferred indirectly from surface pressure measurements until now.

It is interesting to consider that P/S aggregates like those exploited in the present work also exist in the mixed systems that have been studied for decades in the context of molecular adsorption and that are widely used in consumer products. We have shown previously that such aggregates can interact with interfaces by different mechanisms, 16 and that the resulting effects can dominate the interfacial properties.¹⁷ In the present work, the properties of films formed through the explicit exploitation of dissociation and spreading from neutral P/S aggregates have been characterized under static and dynamic conditions for

the first time to show that they are robust and insoluble on the accessed time scales. We conclude that the interfacial properties of oppositely charged polyelectrolyte/surfactant systems in general may be highly influenced by direct aggregate interactions: even in cases where the interfacial properties seem to have reached steady state the system can be far from equilibrium.

Acknowledgements

We thank the ILL for use of FIGARO (DOI: 10.5291/ILL-DATA.9-12-408) and the studentship for AT, the Partnership for Soft Condensed Matter (Grenoble, France) for use of the ellipsometer and Brewster angle microscope, Jutta Toscano and Federica Sebastiani for preliminary measurements, Krisztina Sebestény for laboratory assistance, Simon Wood for technical assistance, and Daniela Ciumac for input into the table-of-content image. This work was supported by the Hungarian Scientific Research Fund (OTKA K100762 & K116629) and by NanoS3 Marie Curie Initial Training Network, funded through the European Union Seventh Framework Programme under grant agreement no. 290251. BAN is grateful to St. Petersburg State University for the financial support (research grant no. 12.38.241.2014).

References

- 1 K. Thalberg and B. Lindman, Polymer-surfactant interactions recent developments, in Interactions of surfactants with polymers and proteins, ed. E. D. Goddard and K. P. Ananthapadmanabhan, CRC Press, Boca Raton, FL, 1993.
- 2 G. Agam, Industrial chemicals: their characteristics and development, Elsevier, Amsterdam, 1994.
- 3 Polymer-Surfactant Systems, ed. J. C. T. Kwak, Marcel Dekker, New York, 1998, vol. 7.
- 4 E. D. Goddard, J. Colloid Interface Sci., 2002, 256, 228.
- 5 A. Asnacios, D. Langevin and J.-F. Argillier, Macromolecules, 1996, 29, 7412.
- 6 D. J. F. Taylor, R. K. Thomas and J. Penfold, Adv. Colloid Interface Sci., 2007, 132, 69.
- 7 E. D. Goddard, Colloids Surf., 1986, 19, 301.
- 8 K. Hayakawa and J. Kwak, in Carionic Surfactants: Physical Chemistry, ed. D. Rubingh and P. M. Holland, Surfactant Science Series, Marcel Dekker, New York, 1991, p. 189.
- 9 K. Kogej, Adv. Colloid Interface Sci., 2010, **158**, 68.
- 10 A. Naderi, P. M. Claesson, M. Bergström and A. Dedinaite, Colloids Surf., A, 2005, 253, 83.
- 11 A. Mezei, R. Meszaros, I. Varga and T. Gilanyi, Langmuir, 2007, 23, 4237.
- 12 A. Mezei, K. Pojjak and R. Mészáros, J. Phys. Chem. B, 2008, **112**, 9693.
- 13 R. A. Campbell, M. Yanez Arteta, A. Angus-Smyth, T. Nylander and I. Varga, J. Phys. Chem. B, 2011, 115, 15202.
- 14 Á. Ábraham, R. A. Campbell and I. Varga, Langmuir, 2013, 29, 11554.
- 15 R. A. Campbell, M. Yanez Arteta, A. Angus-Smyth, T. Nylander and I. Varga, J. Phys. Chem. B, 2012, 116, 7981.

Soft Matter

16 R. A. Campbell, M. Yanez Arteta, A. Angus-Smyth, T. Nylander, B. A. Noskov and I. Varga, *Langmuir*, 2014, **30**, 8664.

- 17 A. Angus-Smyth, C. D. Bain, I. Varga and R. A. Campbell, Soft Matter, 2013, 9, 6103.
- 18 M. Yanez Arteta, R. A. Campbell, E. B. Watkins, M. Obiols-Rabasa, K. Schillén and T. Nylander, *J. Phys. Chem. B*, 2014, **118**, 11835.
- 19 E. Gorter and F. Grendel, Trans. Faraday Soc., 1926, 22, 477.
- 20 E. Hughes and E. K. Rideal, *Proc. R. Soc. London, Ser. A*, 1932, **137**, 62.
- 21 D. Crisp, in Surface Phenomena in Chemistry and Biology, ed. J. F. Danielli, K. G. A. Pankhurst and A. C. Riddiford, Pergamon, New York, 1958.
- 22 R. A. L. Jones and R. W. Richards, *Polymers at Surfaces and Interfaces*, Cambridge University Press, Cambridge, 1999, p. 327.
- 23 N. J. Jain, P.-A. Albouy and D. Langevin, *Langmuir*, 2003, 19, 5680.
- 24 C. Monteux, C. E. Williams, J. Meunier, O. Anthony and V. Bergeron, *Langmuir*, 2004, **20**, 57.
- 25 B. A. Noskov, G. Loglio and R. Miller, *Adv. Colloid Interface Sci.*, 2011, **168**, 179.
- 26 B. M. D. O'Driscoll, E. Milsom, C. Fernandez-Martin, L. White, S. J. Roser and K. J. Edler, *Macromolecules*, 2005, 38, 8785.
- 27 Y. Gao, L. T. Duc, A. Ali, B. Liang, J. T. Liang and P. Dhar, Langmuir, 2013, 29, 3654.
- 28 Y. Gao, M. R. Chowdhury, J. T. Liang and P. Dhar, *J. Appl. Polym. Sci.*, 2015, **132**, 42099.
- 29 L. J. Tong, M. T. Bao, Y. M. Li and H. Y. Gong, Appl. Surf. Sci., 2014, 316, 147.
- 30 Y.-H. Lee, A. Dudek, T.-N. Ke, F.-W. Hsaio and C.-H. Chang, *Macromolecules*, 2008, **41**, 5845.
- 31 K. Tonigold, I. Varga, T. Nylander and R. A. Campbell, *Langmuir*, 2009, 25, 4036.
- 32 S. Manning-Benson, C. D. Bain and R. C. Darton, *J. Colloid Interface Sci.*, 1997, **189**, 109.
- 33 P. X. Li, R. K. Thomas and J. Penfold, *Langmuir*, 2014, 30, 6739.
- 34 R. A. Campbell, H. P. Wacklin, I. Sutton, R. Cubitt and G. Fragneto, *Eur. Phys. J. Plus*, 2011, **126**, 107.
- 35 A. Nelson, J. Appl. Crystallogr., 2006, 39, 273.
- 36 E. Dickinson, D. S. Horne, J. J. S. Phipps and R. M. Richardson, *Langmuir*, 1993, **9**, 242.
- 37 P. M. Saville, P. A. Reynolds, J. W. White, C. J. Hawker, J. M. J. Frechet, K. L. Wooley, J. Penfold and J. R. P. Webster, J. Phys. Chem., 1995, 99, 8283.

- 38 D. J. F. Taylor, R. K. Thomas and J. Penfold, *Langmuir*, 2002, 18, 4748.
- 39 M. Wadsäter, J. B. Simonsen, T. Lauridsen, E. G. Tveten, P. Naur, T. Bjørnholm, H. Wacklin, K. Mortensen, L. Arleth, R. Feidenhans'l and M. Cárdenas, *Langmuir*, 2011, 27, 15065.
- 40 F. Foglia, G. Fragneto, L. A. Clifton, M. J. Lawrence and D. J. Barlow, *Langmuir*, 2014, **30**, 9147.
- 41 H. Fauser, R. von Klitzing and R. A. Campbell, *J. Phys. Chem. B*, 2015, **119**, 348.
- 42 J. R. Lu, R. K. Thomas and J. Penfold, *Adv. Colloid Interface Sci.*, 2000, **84**, 143.
- 43 T. Wallin and P. Linse, Langmuir, 1996, 12, 305.
- 44 S. Sitar, B. Goderis, P. Hansson and K. Kogej, *J. Phys. Chem. B*, 2012, **116**, 4634.
- 45 N. Kristen-Hochrein, A. Laschewsky, R. Miller and R. von Klitzing, *J. Phys. Chem. B*, 2011, **115**, 14475.
- 46 K. Pojják, E. Bertalanits and R. Mészáros, *Langmuir*, 2011, 27, 9139.
- 47 Á. Ábraham, A. Kardos, A. Mezei, R. A. Campbell and I. Varga, *Langmuir*, 2014, **30**, 4970.
- 48 R. Cubitt and J. Stahn, Eur. Phys. J. Plus, 2011, 126, 111.
- 49 J. Perez Gil, *Biochim. Biophys. Acta, Biomembr.*, 2008, **1778**, 1676.
- 50 G. Yang, M. O'Duill, V. Gouverneur and M. P. Krafft, *Angew. Chem.*, *Int. Ed.*, 2014, 54, 8402.
- 51 E. H. Lucasen-Reynders and J. Lucassen, *Adv. Colloid Interface Sci.*, 1970, 2, 347.
- 52 A. G. Bykov, B. A. Noskov, G. Loglio, V. V. Lyadinskaya and R. Miller, *Soft Matter*, 2014, **10**, 6499.
- 53 W. D. Harkins, *The physical chemistry of surface films*, Rheingold, New York, 1952.
- 54 R. v. Klitzing, A. Espert, A. Asnacios, T. Hellweg, A. Colin and D. Langevin, *Colloids Surf.*, A, 1999, 149, 131.
- 55 V. N. Morozov and T. Y. Morozova, *Anal. Chem.*, 1999, 71, 1415.
- 56 R. A. Jain, Biomaterials, 2000, 21, 2475.
- 57 Advances in water treatment and pollution prevention, ed. S. K. Sharma and R. Sanghi, Springer, Dordrecht, 2012.
- 58 C. G. Bell, C. J. W. Breward, P. D. Howell, J. Penfold and R. K. Thomas, *Langmuir*, 2007, 23, 6042.
- 59 A. Bahramanian, R. K. Thomas and J. Penfold, *J. Phys. Chem. B*, 2014, **118**, 2769.
- 60 R. K. Thomas, Lund University, September 2014, *private communication*.